Supporting Information

Custom-tailored solvents engineering for efficient wide-bandgap perovskite solar cells with a wide processing window and low V_{OC} losses

Ruohao Wang,[†a] Jingwei Zhu,[†b] Jiayu You,[b] Hao Huang,[c] Yang Yang,[d] Ruihao Chen,[d] Juncheng Wang,[b] Yuliang Xu,[b] Zhiyu Gao,[b] Jiayue Chen,[a] Bangxin Xu,[a] Bing Wang,[a] Cong Chen,*[b] Dewei Zhao*[b] and Wen-Hua Zhang *[ae]

[a] Yunnan Key Laboratory of Carbon Neutrality and Green Low-carbon Technologies, Yunnan Key Laboratory for Micro/Nano Materials & Technology, Southwest United Graduate School, School of Materials and Energy, Yunnan University, Kunming 650504, China

[b] College of Materials Science and Engineering, Sichuan University & Engineering Research Center of Alternative Energy Materials & Devices, Ministry of Education, Chengdu 610065, China

[c] Guangxi Key Laboratory of Processing for Non-ferrous Metals and Featured Materials & School of Resources, Environment and Materials, Guangxi University, Nanning 530004, China

[d] State Key Laboratory of Solidification Processing, Center for Nano Energy Materials, School of Materials Science and Engineering, Northwestern Polytechnical University and Shaanxi Joint Laboratory of Graphene, Xi'an 710072, China

[e] Southwest United Graduate School, Kunming 650092, China

* Correspondence to: chen.cong@scu.edu.cn, dewei_zhao@hotmail.com and wenhuazhang@ynu.edu.cn.

[†]These authors contributed equally.

Methods

Materials

All materials were purchased from commercial suppliers without special treatment, unless otherwise specified. N,N-dimethylformamide (DMF, 99.8%), dimethyl sulfoxide (DMSO, 99.9%), 1,3-Dimethyl-3,4,5,6-tetrahydro-2(1H)-pyrimidinone (DMPU, 99%), anhydrous ethanol, chlorobenzene (CB, 99.9%), Lead sulfocyanide (Pb(SCN)$_2$, 99.5%) were sourced from Sigma-Aldrich. Isopropanol (IPA, 99.5%) was sourced from J&K Scientific. 1,3-propanediamine dihydriodide (PDAI$_2$, 98%) was sourced from Xi'an Polymer Light Technology Corp. Diethyl carbonate (DEC) was sourced from Damas-beta. Lead iodide (PbI$_2$) and lead bromide (PbBr$_2$) were sourced from TCI. Methylammonium iodide (MAI) and formamidinium iodide (FAI) were sourced from Greatcell Solar Company. Caesium iodide (CsI, 99%) was sourced from Alfa Aesar. 4PADCB was sourced Shanghai Weizhu Chemical Technology Co., Ltd. C$_{60}$ was sourced from Nano-C. Copper (Cu) was sourced from ZhongNuo Advanced Material (Beijing) Technology Co., Ltd. Tetrakis (dimethylamino) tin(IV) (99.9999%) for atomic layer deposited (ALD) SnO$_2$ was sourced from Nanjing Ai Mou Yuan Scientific Equipment.

Perovskite precursor preparation

The FA$_{0.8}$Cs$_{0.15}$MA$_{0.05}$PbI$_{2.4}$Br$_{0.6}$: 1.4 M FA$_{0.8}$Cs$_{0.15}$MA$_{0.05}$PbI$_{2.4}$Br$_{0.6}$ precursor was prepared by dissolving 193.57 mg FAI, 54.56 mg CsI, 451.79 mg PbI$_2$, 11.18 mg MAI, 154.16 mg PbBr$_2$ and 3.5 mg Pb(SCN)$_2$ in 1 ml DMF:DMSO (v:v=8:2, control) or DMF:DMSO:DMPU (v:v:v=8:1.7:0.3, target) and stirred overnight.

Device fabrication

The glass substrate coated with ITO (25×25 mm, 10 Ω sq^{-1}) was ultrasonically cleaned for 15 min with deoxidizing agent, deionized water and ethanol in sequence. ITO glass substrate was dried with nitrogen stream and treated with ultraviolet-ozone for 15 min. Then 80 µl solvent of 4PADCB (dissolved in ethanol, 0.5 mg ml^{-1}) was spin-coated on the ITO substrate at 3000 rpm for 20 s, followed by annealing at 100 °C

for 10 min. The perovskite film was prepared by one-step spin-coating (step 1 at 500 rpm for 2 s and 4000 rpm for 60 s) with 80 µL precursor dripped on 4PADCB substrate. The antisolvent dripping time of second step was determined according to different requirements. Then the wet perovskite film was quickly placed on the hot table and annealed at 70°C for 2 min and 100°C for 8 min. After the prepared perovskite film was cooled to normal temperature, 80 µL solution of $PDAI_2$ (in mixed IPA:CB = 1:1, 1 mg mL^{-1}) was added to the surface of the perovskite at 3000 rpm for 30 s, and then annealed at 100 °C for 10 min. Then devices were obtained by vacuum evaporation for 20 nm C_{60}, 5 nm BCP, and 100 nm Cu in a multisource evaporation chamber at 5×10^{-4} Pa.

Film and Device Characterization

X-ray diffraction (XRD) patterns of perovskite films treated with different solvent systems were performed by Shimazu XRD-6100 diffractometer. SEM images were obtained by Hitachi Regulus-8230. In-situ PL spectra were obtained using an Ocean Optics' spectrometer with 365 nm UV exciter. Absorbance spectra were obtained by UV-vis spectrophotometer (PerkinElmer Lambda 950). PL and TRPL were measured by FLS980 (Edinburgh). By focusing on the perovskite film, the detector collects spectral signals. Finally, using professional software to process the data, the plane PL mapping was drawn. Surface AFM and KPFM of perovskite films were obtained by Bruker Nano Inc DI Multi Mode 8. UPS were obtained by ESCALAB 250Xi (Thermo Fisher Scientific,). EIS and C-V were recorded by the electrochemical workstation (IVIUMSTAT). Frequency of EIS measurement was changed from 10^6 Hz to 1000 Hz at the bias of 1.0 V with an amplitude of 10 mV. Frequency of C-V measurement was fixed at 1000 Hz with the voltage range of 0 V to 1.1 V. The MPP tracking was recorded by white LED simulator (Weina Bonuo new materials Co., Ltd., Qingdao) equivalent to 1 sun (100 mW cm^{-2}) at the air. J-V curves of devices were obtained by Keysight B2901A under AM1.5G illumination (Enlitech, SS-F5-3A) with an active area of 0.0576 cm^2 in an N_2-filled glove box. Before all J-V measurements, solar simulator was calibrated with a silicon reference cell (Enlitech, SRC-00205). The scan rate for J-V measurement was 100 mV s^{-1}, with delay time of 100 ms and voltage step of 10 mV.

The light intensity dependence of V_{OC} was obtained by measuring J-V curves under different illumination intensities. The EQE was recorded by a solar cell quantum efficiency measurement system (QE-R, Enlitech) under monochromatic light ranging from 300 nm to 800 nm with a 10 nm increment and a chopper frequency of 210 Hz. The dark J-V and SCLC was measured by Keysight B2901A source meter under dark conditions. External electroluminescence quantum efficiency (EQE$_{EL}$) measurement was measured on ELCT-3010 (Enlitech) with a step of 0.1 V. In-situ PL measurements were conducted using an Ocean Optics' spectrometer equipped with 365 nm UV exciter. The PL signal of the perovskite films is detected by a receiver positioned at a distance of 1 cm from the sample during the spin-coating and annealing. The annealing temperature was set at 70 °C.
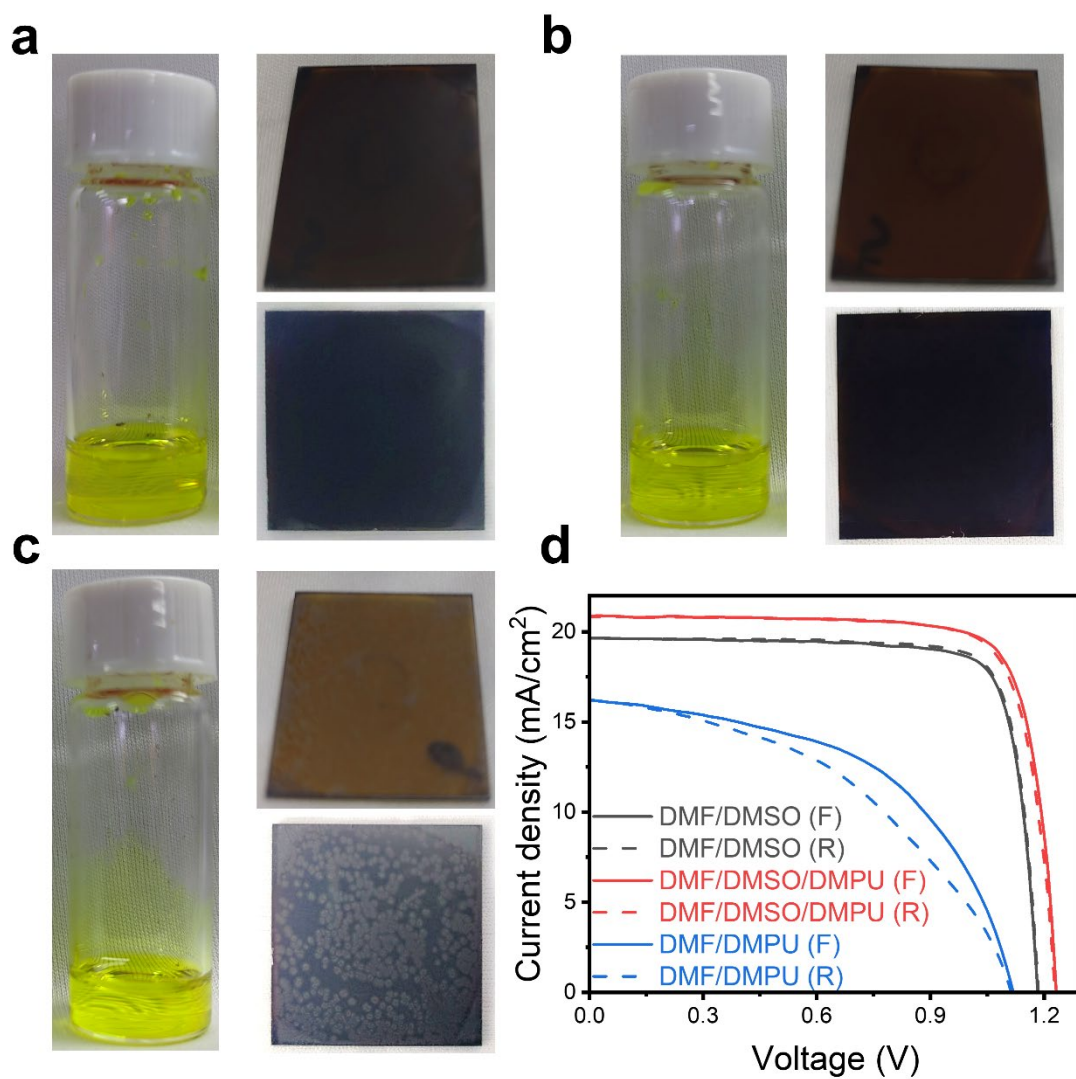
Supplementary Fig. S1-S13

Fig. S1. Perovskite precursor of different solvent system and corresponding perovskite film after and before annealing, (a) DMF/DMSO, (b) DMF/DMSO/DMPU, (c) DMF/DMPU. (d) Corresponding *J-V* curves of the devices.
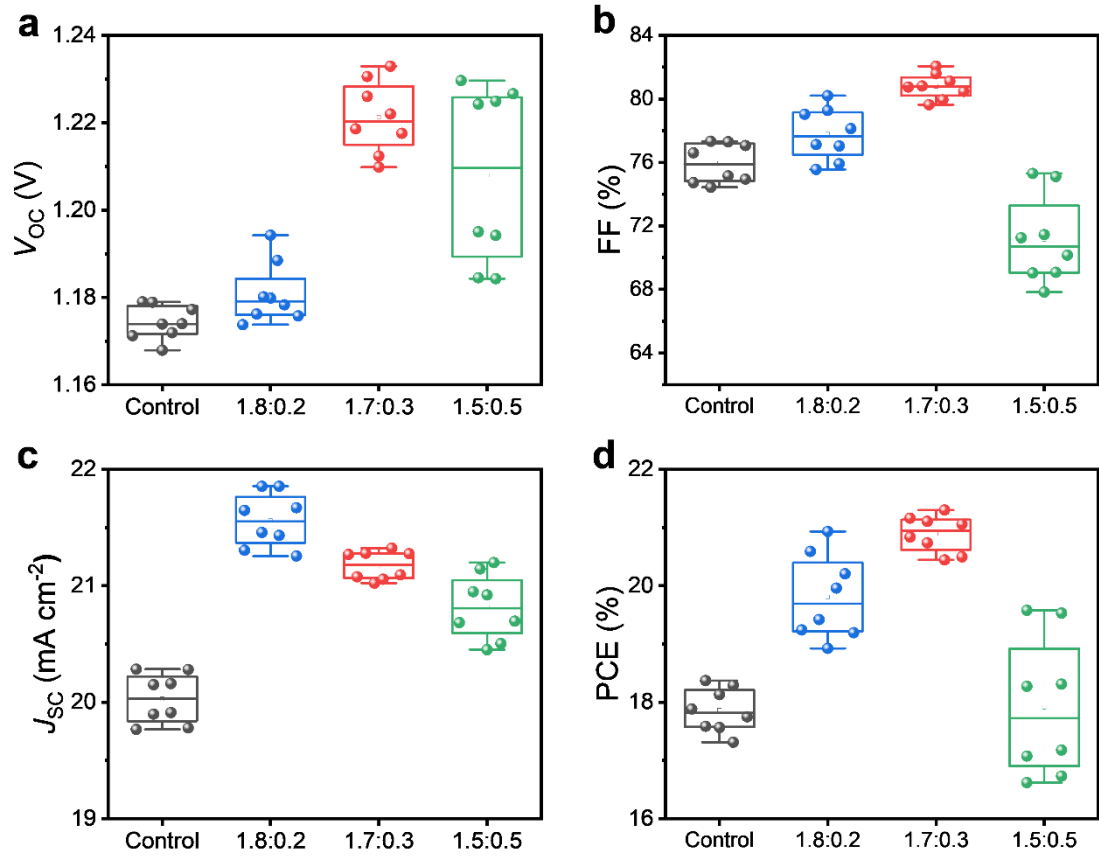
Fig. S2. Statistics of photovoltaic parameters of control and target devices with different volume ratio: (a) V_{OC}, (b) FF, (c) J_{SC}, and (d) PCE.
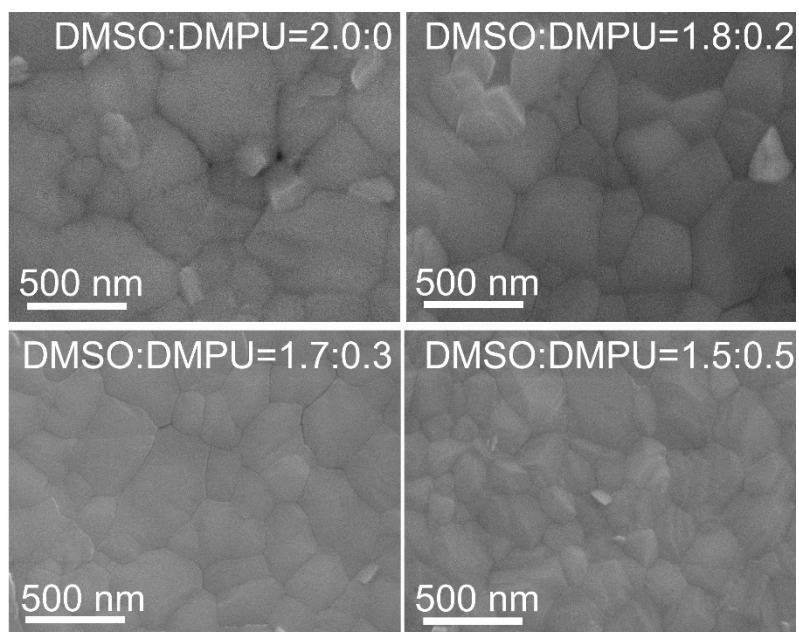
Fig. S3. SEM images of perovskite films with different replaced volume ratio.
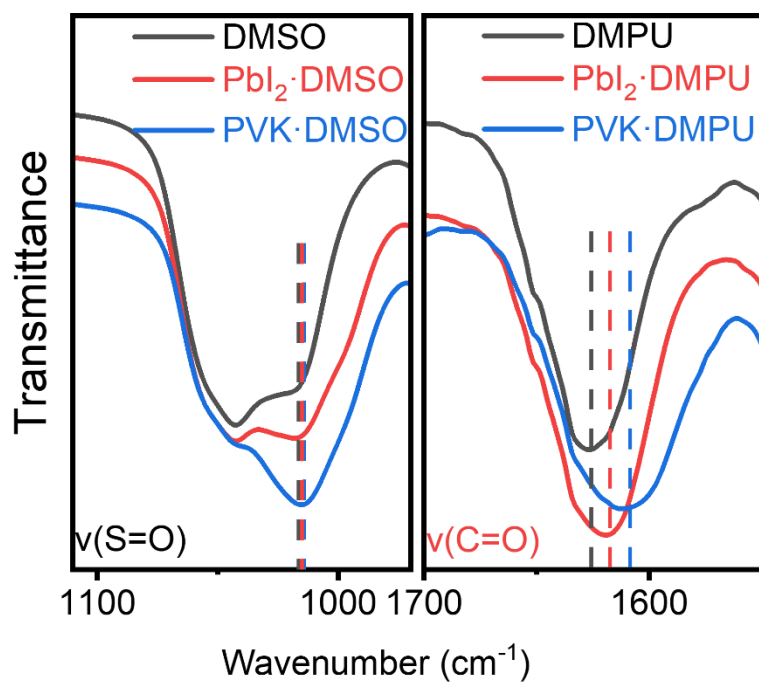
Fig. S4. FTIR spectra of DMSO, DMSO with PbI_2, DMSO with perovskite components (PVK) in the regions of 1100-970 cm^{-1} and the FTIR spectra of DMPU, DMPU with PbI_2, DMPU with PVK in the region of 1700-1550 cm^{-1}.
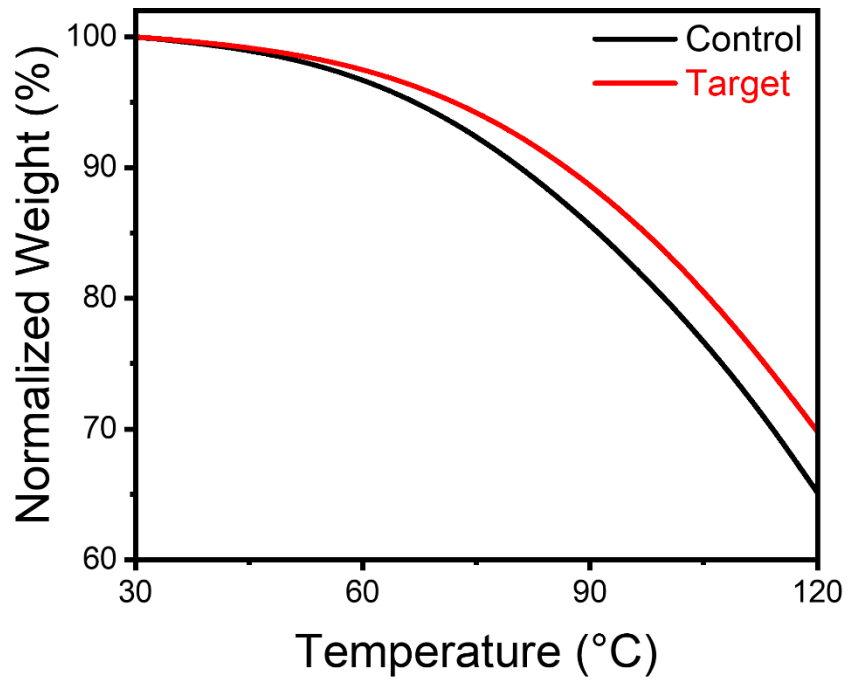
Fig. S5. TGA curves of control and target perovskite precursor solution.
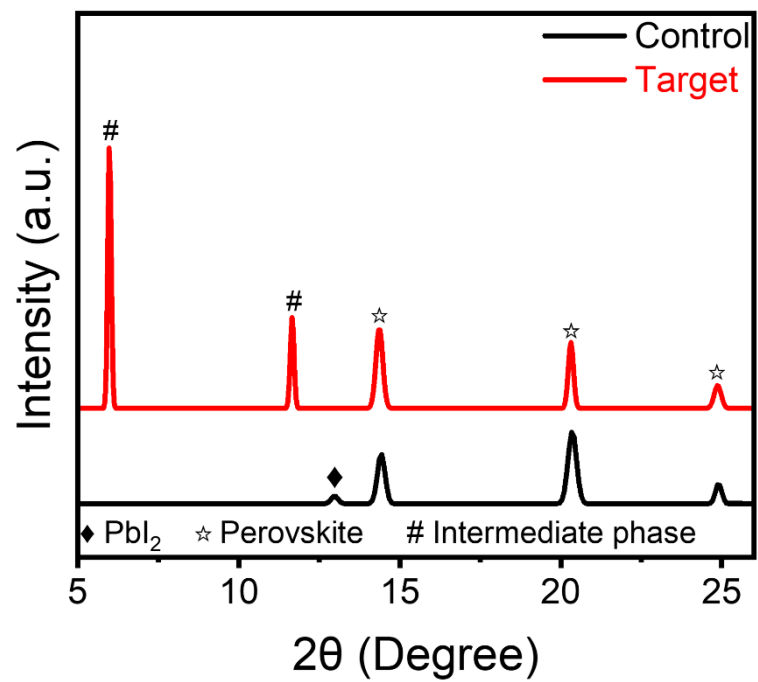
Fig. S6. XRD patterns of control and target perovskite wet film after antisolvent dripping.
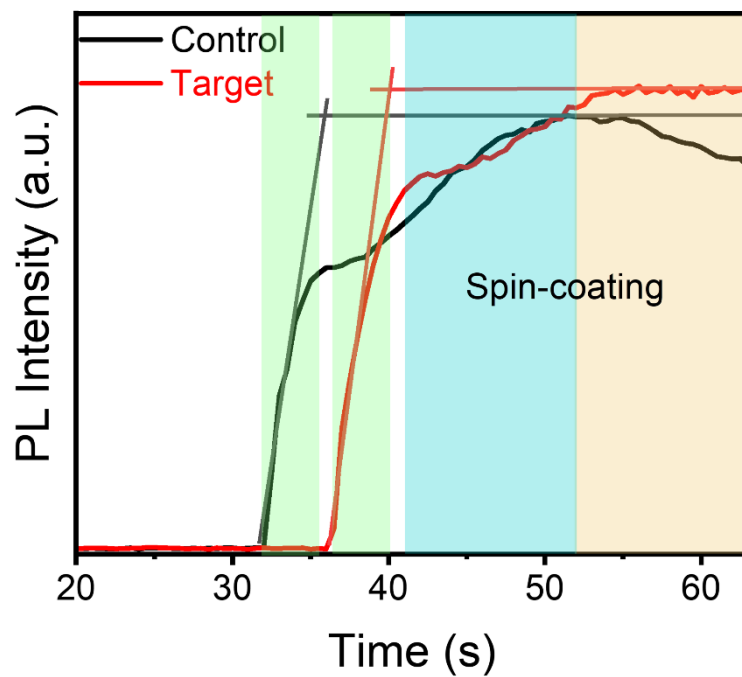
Fig. S7. PL intensity trend of control and target films with time during spin-coating process.
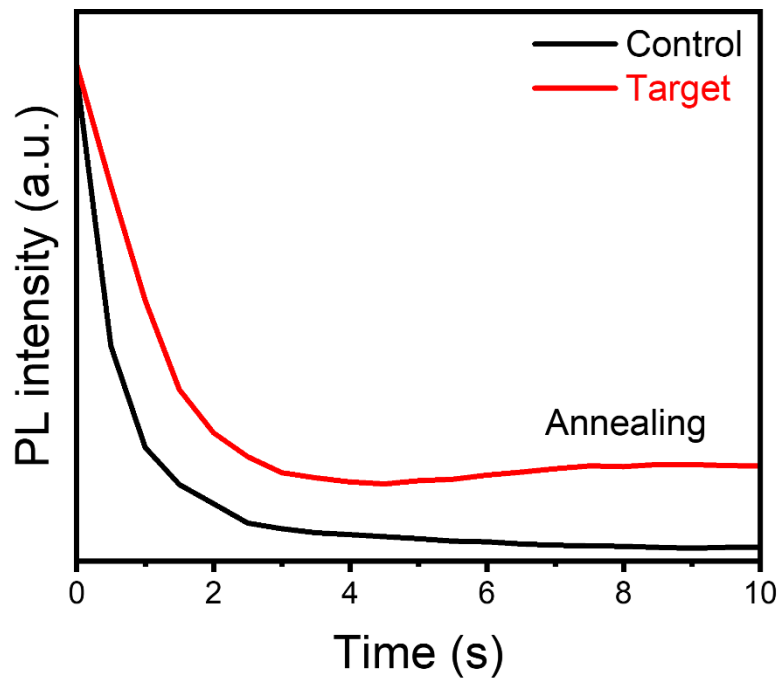
Fig. S8. PL intensity trend of control and target films with time during annealing process.
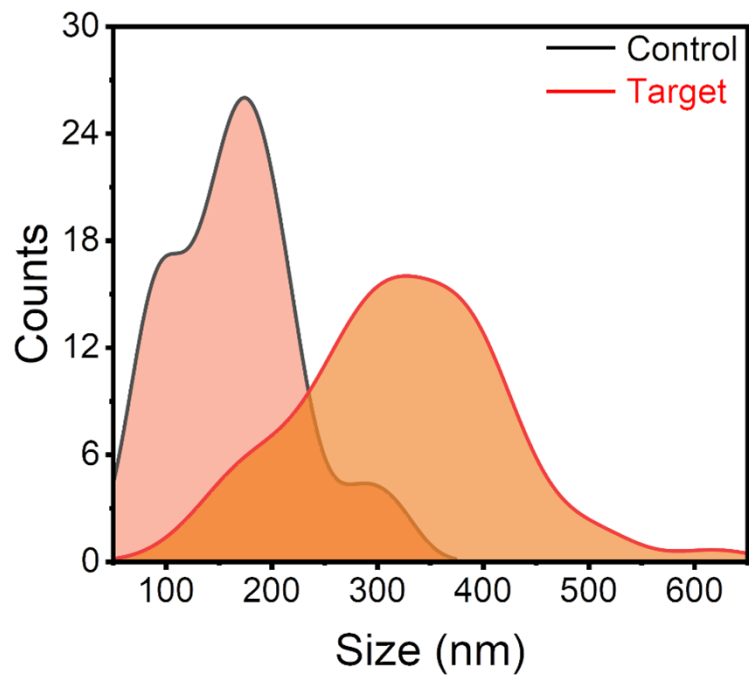
Fig. S9. Grain size distribution diagram of control and target films.
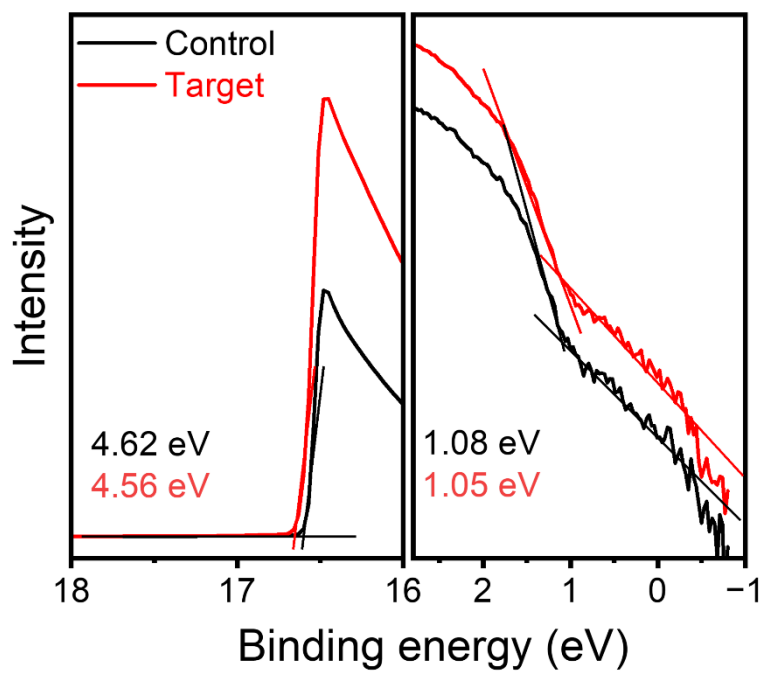
Fig. S10. UPS spectra of control and target perovskite films.
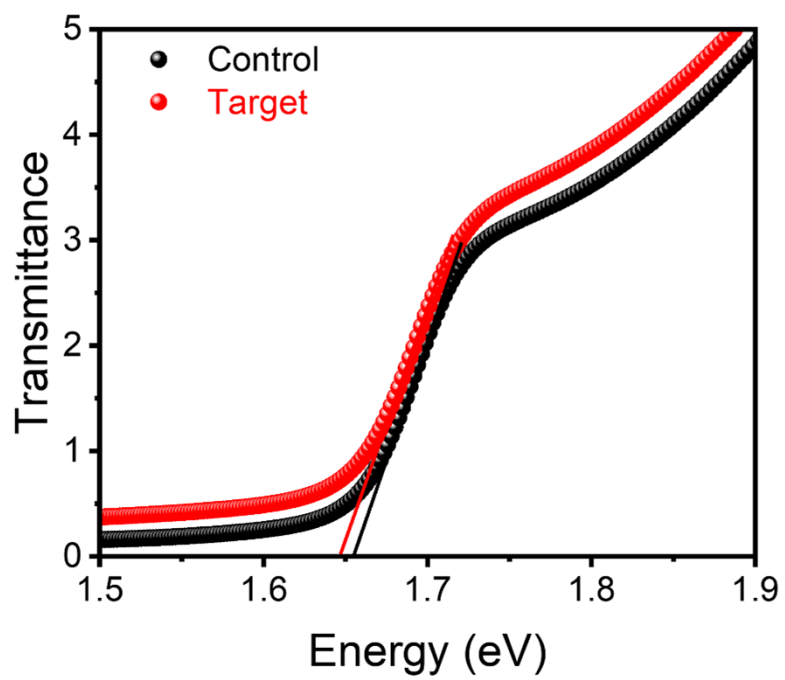
Fig. S11. UV-vis absorbance traces of control and target perovskite films.
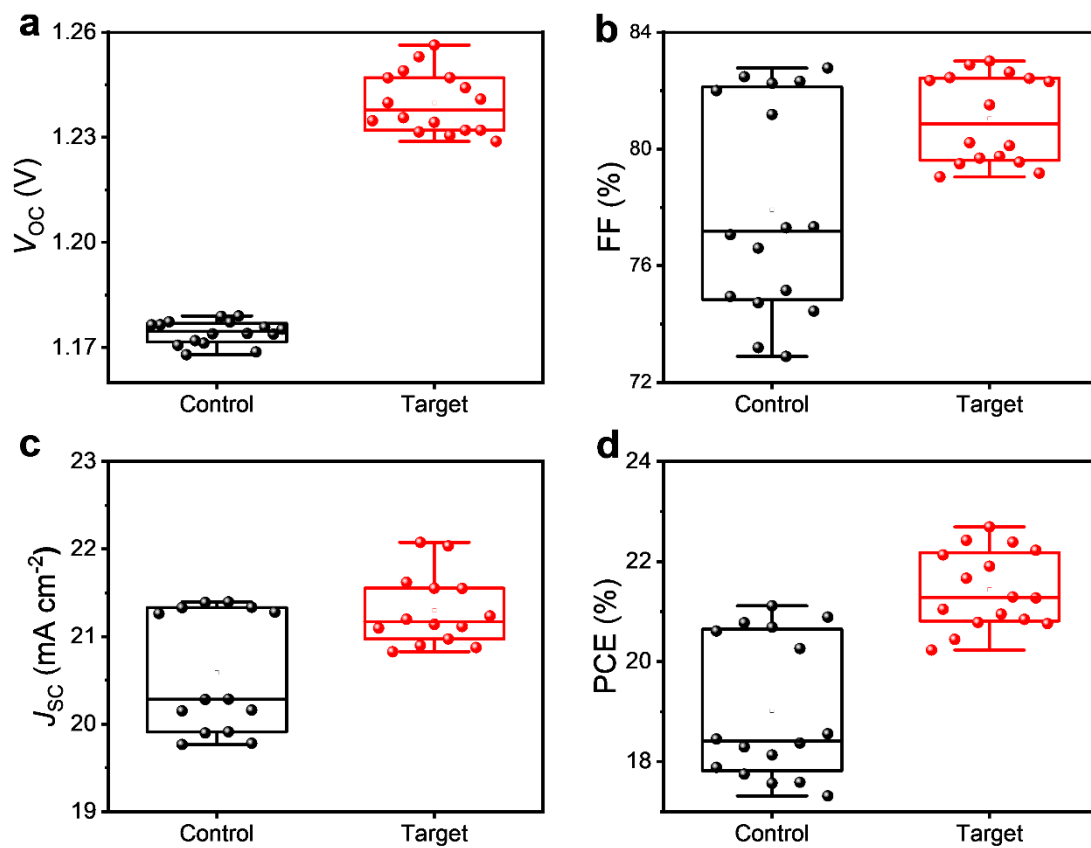
Fig. S12. Statistics of photovoltaic parameters of control and target devices, (a) V_{OC}, (b) FF, (c) J_{SC}, and (d) PCE.
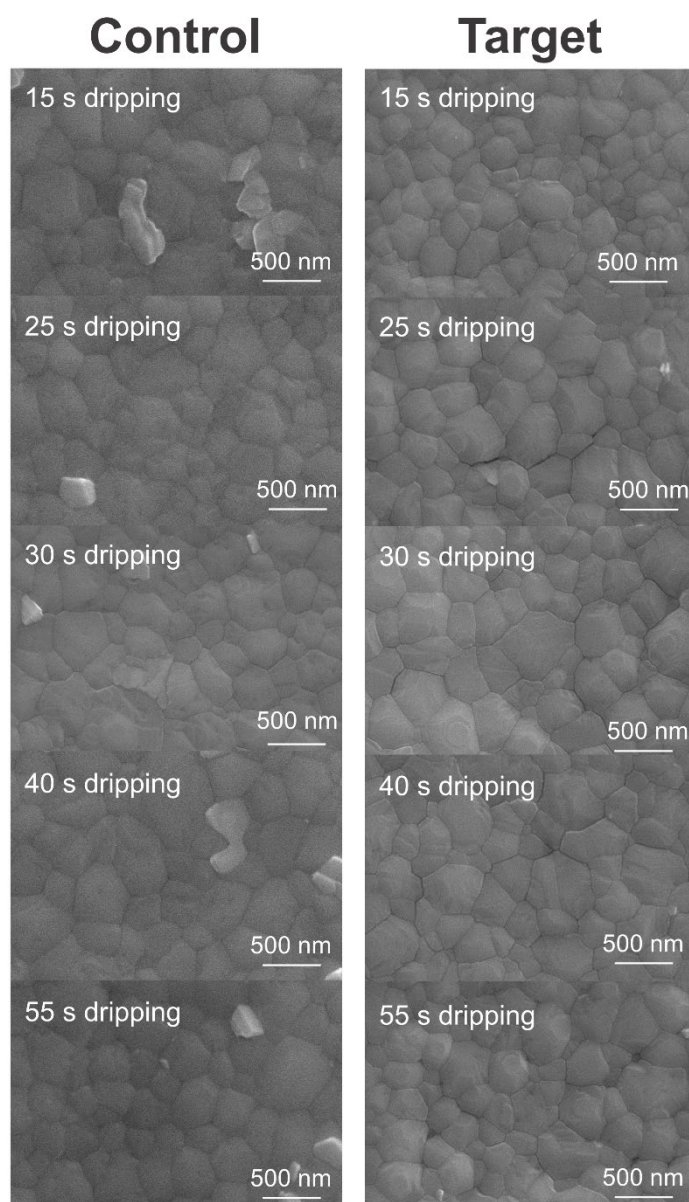
Fig. S13. SEM images of control and target perovskite films at different antisolvent dripping times.

Supplementary Tables

Table S1. Summary on photovoltaic performance of PSCs based on different solvent system.

Sample		V_{OC} (V)	J_{SC} (mA cm^{-2})	FF (%)	PCE (%)
DMF/DMSO	Forward	1.18	19.8	79.1	18.5
	Reverse	1.18	19.8	79.3	18.6
DMF/DMSO/DMPU	Forward	1.23	20.9	80.1	20.6
	Reverse	1.23	20.9	81.0	20.8
DMF/DMPU	Forward	1.12	16.2	60.1	10.9
	Reverse	1.12	16.2	50.3	9.1

Table S2. Carrier lifetimes of control and target perovskite films on bare glass from TRPL decays via bi-exponential fitting.

TRPL	τ_1 (ns)	A_1	τ_2 (ns)	A_2	τ_{ave} (ns)
Control	60.6	0.122	121	0.878	113.6
Target	75.2	0.165	417	0.835	360.6

Table S3. Summary on main photovoltaic parameters of control and target devices.

Sample		V_{OC} (V)	J_{SC} (mA cm^{-2})	FF (%)	PCE (%)
Control	Forward	1.185	20.92	78.7	19.5
	Reverse	1.177	20.90	78.4	19.3
Target	Forward	1.253	20.97	82.4	21.7
	Reverse	1.256	21.00	83.0	21.9

Table S4. EIS fitting parameters of control and target perovskite devices.

Sample	R_s (Ω)	R_{rec} $(k\Omega)$	C_{rec} (F)
control	22.39	114.3	1.7×10^{-8}
target	23.64	1104	1.2×10^{-8}

Table S5. Summary on the photovoltaic parameters of WBG (1.65-1.68 eV) PSCs extracted from recent literature on all PSCs.

Year	Type	E_g (eV)	V_{OC} deficit (V)	V_{OC} (V)	FF (%)	J_{SC} (mA/cm²)	PCE (%)	Ref.
2020	p-i-n	1.67	0.45	1.22	83.2	20.2	20.4	[1]
2021	n-i-p	1.67	0.47	1.20	79.80	20.03	19.10	[2]
2022	p-i-n	1.66	0.44	1.22	76.90	20.06	19.30	[3]
2022	p-i-n	1.65	0.42	1.23	83.80	21.2	21.9	[4]
2023	p-i-n	1.68	0.441	1.239	82.50	21.16	21.63	[5]
2023	p-i-n	1.68	0.42	1.26	81.60	21.60	22.19	[6]
2023	p-i-n	1.65	0.41	1.24	81.77	21.29	21.55	[7]
2023	p-i-n	1.67	0.408	1.262	82.7	20.9	21.8	[8]
2023	p-i-n	1.68	0.432	1.248	84.4	20.82	21.93	[9]
2023	p-i-n	1.67	0.41	1.26	82.6	20.5	21.3	[10]
2023	p-i-n	1.65	0.39	1.25	79.48	21.93	21.80	[11]
2023	p-i-n	1.68	0.40	1.28	-	-	21.5	[12]
2023	p-i-n	1.67	0.43	1.24	85.5	21.7	23.1	[13]
2023	p-i-n	1.67	0.398	1.272	82.00	21.07	22.00	[14]
	p-i-n	1.65	0.394	1.256	83.00	21.00	21.90	This work

References

1   J. Xu, C. C. Boyd, Z. J. Yu, A. F. Palmstrom, D. J. Witter, B. W. Larson, R. M. France, J. Werner, S. P. Harvey, E. J. Wolf, W. Weigand, S. Manzoor, M. van Hest, J. J. Berry, J. M. Luther, Z. C. Holman and M. D. McGehee, *Science*, 2020, **367**, 1097-1104.

2   X. Fu, T. He, S. Zhang, X. Lei, Y. Jiang, D. Wang, P. Sun, D. Zhao, H.-Y. Hsu, X. Li, M. Wang and M. Yuan, *Chem*, 2021, **7**, 3131-3143.

3   J. Zhao, A. S. R. Chesman, J. Yan, L. J. Sutherland, J. Jasieniak, J. Lu, W. Mao and U. Bach, *ACS Appl. Mater. Inter.*, 2023, **15**, 18800-18807.

4   G. Yang, Z. Ni, Z. J. Yu, B. W. Larson, Z. Yu, B. Chen, A. Alasfour, X. Xiao, J. M. Luther, Z. C. Holman and J. Huang, *Nat. Photonics*, 2022, **16**, 588-594.

5   N. Yan, Y. Gao, J. Yang, Z. Fang, J. Feng, X. Wu, T. Chen and S. Liu, *Angew. Chem. Int. Ed.*, 2023, **62**, e202216668.

6   Z. Song, J. Yang, X. Dong, R. Wang, Y. Dong, D. Liu and Y. Liu, *Nano Lett.*, 2023, **23**, 6705-6712.

7   G. Su, R. Yu, Y. Dong, Z. He, Y. Zhang, R. Wang, Q. Dang, S. Sha, Q. Lv, Z. Xu, Z. Liu, M. Li and Z. a. Tan, *Adv. Energy Mater.*, 2023, 2303344.

8   Z. Liu, H. Li, Z. Chu, R. Xia, J. Wen, Y. Mo, H. Zhu, H. Luo, X. Zheng, Z. Huang, X. Luo, B. Wang, X. Zhang, G. Yang, Z. Feng, Y. Chen, W. Kong, J. Gao and H. Tan, *Adv. Mater.*, 2023, 202308370.

9   E. Aydin, E. Ugur, B. K. Yildirim, T. G. Allen, P. Dally, A. Razzaq, F. Cao, L. Xu, B. Vishal, A. Yazmaciyan, A. A. Said, S. Zhumagali, R. Azmi, M. Babics, A. Fell, C. Xiao and S. De Wolf, *Nature*, 2023, **623**, 732-738.

10   G. Wang, J. Zheng, W. Duan, J. Yang, M. A. Mahmud, Q. Lian, S. Tang, C. Liao, J. Bing, J. Yi, T. L. Leung, X. Cui, H. Chen, F. Jiang, Y. Huang, A. Lambertz, M. Jankovec, M. Topič, S. Bremner, Y.-Z. Zhang, C. Cheng, K. Ding and A. Ho-Baillie, *Joule*, 2023, **7**, 2583-2594.

11   Z. Li, X. Li, X. Chen, X. Cui, C. Guo, X. Feng, D. Ren, Y. Mo, M. Yang, H. Huang, R. Jia, X. Liu, L. Han, S. Dai and M. Cai, *Joule*, 2023, **7**, 1363-1381.

12   S. Mariotti, E. Köhnen, F. Scheler, K. Sveinbjörnsson, L. Zimmermann, M. Piot, F. Yang, B. Li, J. Warby, A. Musiienko, D. Menzel, F. Lang, S. Keßler, I. Levine, D. Mantione, A. Al-Ashouri, M. S. Härtel, K. Xu, A. Cruz, J. Kurpiers, P. Wagner, H. Köbler, J. Li, A. Magomedov, D. Mecerreyes, E. Unger, A. Abate, M. Stolterfoht, B. Stannowski, R. Schlatmann, L. Korte and S. Albrecht, *Science*, 2023, **381**, 63-69.

13   S. Li, Z. Zheng, J. Ju, S. Cheng, F. Chen, Z. Xue, L. Ma and Z. Wang, *Adv. Mater.*, 2023, 202307701.

14   L. Qiao, T. Ye, T. Wang, W. Kong, R. Sun, L. Zhang, P. Wang, Z. Ge, Y. Peng, X. Zhang, M. Xu, X. Yan, J. Yang, X. Zhang, F. Zeng, L. Han and X. Yang, *Adv. Energy Mater.*, 2023, 2302983.